RESEARCH ARTICLE

Surface modification of cellulose nanofiber aerogels using phthalimide

Sima Sepahvand[1] | Mehdi Jonoobi[1] | Alireza Ashori[2] | Florent Gauvin[3] |
H.J.H. Brouwers[3] | Qingliang Yu[3]

[1]Department of Wood and Paper Science and Technology, Natural Resources Faculty, University of Tehran, Tehran, Iran

[2]Department of Chemical Technologies, Iranian Research Organization for Science and Technology (IROST), Tehran, Iran

[3]Department of the Built Environment, Eindhoven University of Technology, Eindhoven, The Netherlands

Correspondence
Mehdi Jonoobi, Department of Wood and Paper Science and Technology, Natural Resources Faculty, University of Tehran, Tehran, Iran.

Email: mehdi.jonoobi@ut.ac.ir
Alireza Ashori, Department of Chemical Technologies, Iranian Research Organization for Science and Technology (IROST), Tehran, Iran.
Email: ashori@irost.ir

Qingliang Yu, Department of the Built Environment, Eindhoven University of Technology, Eindhoven, The Netherlands.
Email: q.yu@bwk.tue.nl

Funding information
Iran Nanotechnology Initiative Council; University of Tehran; Eindhoven University of Technology

Abstract

The present work studied the possibility of using phthalimide for surface modification of cellulose nanofibers (CNF). The modification was carried out in 96/4 (v/v) water/acetic acid with CNF to phthalimide ratio of 1:0, 1:0.5, 1:1, and 1:1.5 wt%, respectively. Morphological, physical, chemical, and thermal properties of prepared aerogels were characterized by scanning electron microscopy, transmission electron microscopy, X-ray diffraction spectroscopy, and thermogravimetric analysis. The mechanical characterization such as the stress-strain behavior was measured by compression testing. The results showed that surface modification and addition of phthalimide increased the surface area and pore volume but decreased the overall pores size. The presence of phthalimide onto CNF was confirmed by attenuated total reflectance-Fourier transform infrared spectroscopy as the characteristic peaks of NH_2, C—N, and ester bonding (COO^-) appeared. Since more energy is needed for breaking hydroxyl bonds than ionic bonds, by taking into account the reduced hydrogen bonds as the result of the chemical modification, the thermal stability of the CNF-Ph is lower than the pure CNF aerogel. Besides, the modulus of elasticity increased that could be due to the high densities.

KEYWORDS
cellulose nanofiber aerogel, mechanical properties, phthalimide, surface chemical modification

1 | INTRODUCTION

Cellulose as the most abundant biopolymers on earth occurs in wood, cotton, hemp, and other plant-based material and serving as the dominant reinforcing phase in plant structures.[1] Almost any biomaterials compose of approximately 20 to 50 wt% cellulose that consists of a linear homopolysaccharide composed of β-D-glucopyranose units linked together by "glycosidic" link.[2] The —OH group linked to the C-6 is a primary alcohol which allows modification of the cellulose.[3]

Concerning the application and end users, in different sector and industries including biomedical (wound dressing, bone, cartilage and dental restoration, drug delivery, and cancer treatment), as a binder and urea formaldehyde (UF) modifier for fiberboards, as CO_2 absorber, as air, water and cigarette filters, and so on, nanocellulose has been employed.

Feasibility of using cellulose nanofibers (CNF) as the sole binder in a "no-added formaldehyde binding process" for particleboard manufacture was first introduced by the University of Maine.[4] Cellulose hydrogels, for example, are used for chromatographic columns[5,6] or as modified membranes for wastewater cleaning.[7] Up to now, the main industrial/laboratory nanomaterials made out of cellulose are CNF, nanocrystalline cellulose (CNC), and bacterial cellulose.[8] Using nanocellulose in environmental remediation has recently drawn attention because of its great potential for a new generation of nanostructured materials from renewable resources.[2] However, in most cases, nanocellulose needs to undertake a surface modification/fictionalization to harness its great potential. This could be done by employing different strategies of surface modification involving the chemistry of the hydroxyl function.[9] In specific term, surface modification is mandatory to enhance and/or introduce new ability to CNF such as ionizable, ionic, or complexing sites on the surface on which the metal is going to be adsorbed.[10] Many reactions could be involved in modifying the surface of nanocellulose including coupling agents.[11] Different reagents can be used to modify the surface of nanocellulose in order to help better a dispersion of cellulose in the nonpolar polymer matrix and increases the interfacial bonding (e.g., silane and titanate coupling agents).[12,13] Phthalimide (1,3-dihydro-1,3-dioxoisoindole) has been employed to modify talc particle surface in order to improve its physical, mechanical, and optical properties of deinked pulp.[14–16] Carboxylic sulfate and amine-based derivatives are among the most prevalent groups generated to boost the adsorption capacity. These groups can be introduced either during the preparation of nanocellulose or through surface modification of the nanofibers.[17] Khanjanzadeh et al.[12] have recently conducted a study on surface modification of CNC using 3aminopropyltriethoxysilane to tailor its properties as UF resin modifier, and they found that the modified resin had higher mechanical and physical properties and lower formaldehyde emission in comparison to unmodified counterparts.[13] Nevertheless, there is still lack of research on utilization of phthalimide as a coupling agent modifier for CNF in the production of adsorbent.

The main objective of this research was CNF chemical modification with phthalimide, to substitute OH groups of CNF with amino groups of phthalimide. The chemical, thermal, and morphology characteristics of Ph-CNF were determined by scanning electron microscopy (SEM), attenuated total reflectance-Fourier transform infrared (ATR-FTIR) spectroscopy, X-ray diffraction (XRD) spectroscopy, X-ray photoelectron spectroscopy, transmission electron microscopy (TEM), and thermogravimetric analysis (TGA). Also, the mechanical property was carried out by compression testing.

2 | EXPERIMENTAL

2.1 | Materials

Birch kraft pulp, kindly provided by SCA Munksund AB (Piteå, Sweden), was used as raw material for the fibrillation process of CNF. Phthalimide (1,3-dihydro-1,3-dioxisoindole; $C_6H_4[CO]_2NH$) was used for CNF modification and was provided from Merck (Germany). Acetic acid (99.5%) was supplied by Sigma-Aldrich.

2.2 | Preparation of cellulose nanofibers

A shear mixer (Silverson L4RT; Silverson Machines Ltd., England) was used to disperse the kraft pulp suspension (2 wt% concentration) prior to the grinding process. The grinding stones were set to contact mode after the initial feeding of the suspension and gradually adjusted until reaching 90 μm (negative). The stones used were coarse silicon carbide, and the rotor speed was set to 1500 rpm. Ultrafine friction grinder MKZA10-20J (Masuko Sangyo Co., Japan) was used to mechanically separate cellulose fibers to nanosize. The grinding was stopped after gel formation with maximum viscosity was reached.

2.3 | Modification of cellulose nanofibers

Phthalimide powder was added to a mixture of water/acetic acid (96/4 [v/v]) with a ratio of 0.5, 1.0, and 1.5 wt%. Since phthalimide is sensitive to direct heating, it was placed inside glycerol oil and under continuous stirring at 80°C for 24 hr. Then, CNF gel was prepared with a concentration of 1 wt% and stirred at 480 rpm for 3 hr at room temperature. Subsequently, phthalimide was added to CNF gel and was stirred at 65°C for 3 hr. The pH of the solution was set at 4. The CNF-phthalimide solution was centrifuged at 2500 rpm for 10 minutes in order to remove the excess of phthalimide that was not grafted onto the CNF. A Teflon mold (with 30 mm diameter and 40 mm length) was mounted on a cylindrical metal base of copper with 100 mm height and 40 mm diameter. The diluted solution was poured in the mold, then 30 mm from its bottom was placed in liquid N_2 at the temperature of −196°C. Finally, the frozen sample was dried in a freeze dryer (Alpha 1-4 LD plus from Christ) under following conditions: ice condenser = −57°C; vacuum ≤0.1 mbar; time = 48 hr. The resulting materials are referred to as CNF-Ph1.5, CNF-Ph1.0, and CNF-Ph0.5, and pure CNF was used as the control sample (Figure 1).

2.4 | Characterizations
2.4.1 | Scanning electron microscopy

The morphology of CNF and CNF-Ph aerogels was observed using a BSE detector in a SEM (Phenom ProX;
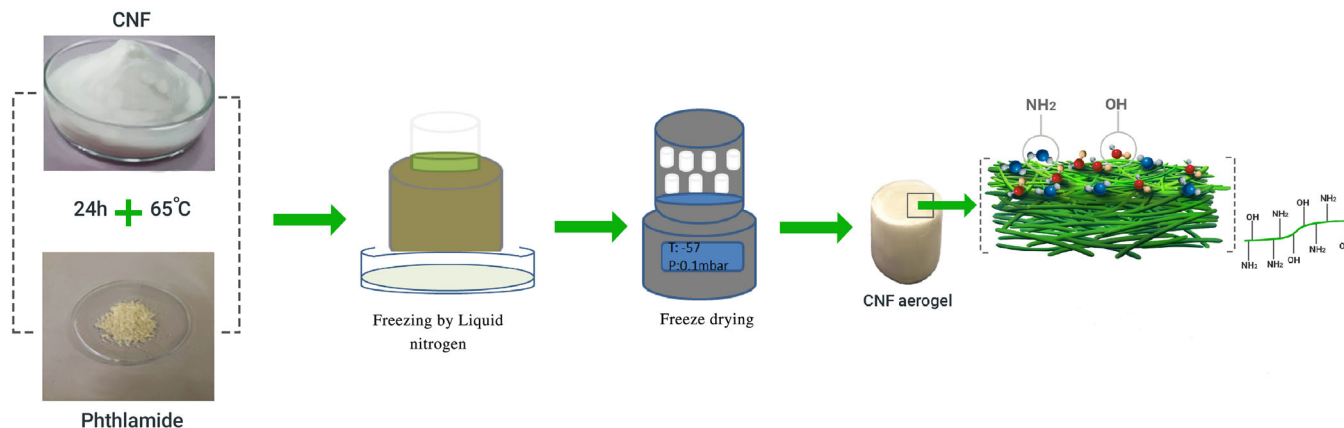
FIGURE 1 Schematic of the modification and fabrication of CNF aerogel [Color figure can be viewed at wileyonlinelibrary.com]

Eindhoven, Netherlands) at an accelerating voltage 10 kV. All samples were sputtered-coated (2 minutes and 25 mA) with a gold layer of approximately 15 nm in thickness.

2.4.2 | Transmission electron microscopy

Aqueous suspensions (0.1 w/w%) of both CNF and CNF-Ph were prepared for TEM analysis. The samples were 100× diluted in water. A drop (10 μL) of aqueous suspension was deposited on a 200 mesh Cu grid covered with a continuous carbon film. The morphology of CNF and CNF-Ph was observed using a FEI Tecnai 20 Sphera (FEI Company, Eindhoven, Netherlands) instrument with a LaB6 filament, operated at an accelerating voltage of 200 kV.

2.4.3 | Zeta potential measurement

Zeta potentials of concentration equalized to diluted suspensions CNF and CNF-Ph to see their charge, and hence, stability was measured with a Zetasizer Nano ZS (Malvern instruments, Malvern, UK).

2.4.4 | Density

The apparent densities of CNF-Ph (ρ_a) were calculated by measuring the mass and volume of each singular aerogel. The weight of an aerogel was measured using analytical balance (readability 0.0001 g, Analytical Balance; Mettler Toledo, Ohio).

2.4.5 | Attenuated total reflectance-Fourier transform infrared

CNF and CNF-Ph aerogels and phthalimide were analyzed with a Perkin Elmer Frontier spectrometer (Spectrum 400 FTIR) using ATR method (GladiATR) to see if grafting

happens. Spectra were obtained by measuring the 400 to 4000 cm^{-1} range at a resolution of 4 cm^{-1}.

2.4.6 | X-ray diffraction

The crystallinity of the CNF was measured using a Bruker AXS X-ray diffractometer with a Co-Kα tube (model D2 PHASER; Bruker, Massachusetts) with wavelength of 0.179 nm. Samples were scanned in 2θ ranges varying from 10° to 50°. The crystallinity index (CrI) was calculated for each sample using the following equation[18]:

$$Xc = \frac{I_{002} - I_{am}}{I_{002}} \times 100 \tag{1}$$

where I_{002} is the maximum intensity of crystallinity of diffraction peak and I_{am} is the intensity scattered by amorphous part of the sample.

2.4.7 | Thermogravimetric analysis

For determination of the materials response in different temperatures and to see the effect of modification on thermal behavior, TGA (Ta Instruments Q500) was carried out. CNF and CNF-Ph aerogel samples were heated from 40°C to 600°C at a heating rate of 10°C per minute under nitrogen with a flow rate of 50 mL/min. The weight of aerogel samples used for the tests was between 10 and 12 mg.

2.4.8 | Mechanical testing

CNF and CNF-Ph aerogels with a cylindrical shape (diameter = 28 mm; height = 12 mm) were tested in compression mode in a MTS Criterion (model 42) equipped with a load cell of 200 N at a speed of 1 mm/min to $\varepsilon = 80\%$ of its original height. Three specimens were tested for each treatment.
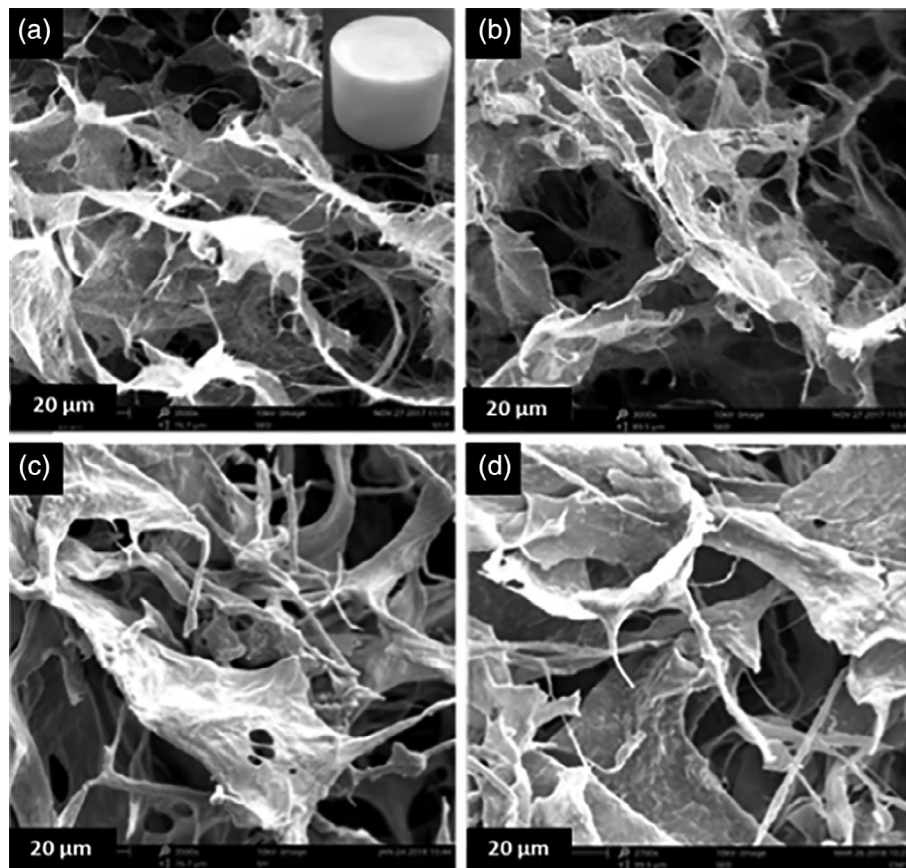
FIGURE 2 a, SEM of an CNF. b, CNF-Ph0.5. c, CNF-Ph1.0. d, CNF-Ph1.5

2.4.9 | Statistical analysis

All the data were subjected to analysis of variance (ANOVA), and the difference between mean was evaluated by Duncan's multiple range test at a confidence level of 95%. The SPSS statistic program (version 20.0) was used for data analysis.

3 | RESULTS AND DISCUSSION

3.1 | Microstructure

The morphological characteristics of the CNF and CNF-Ph aerogels were investigated with SEM, and the micrographs are displayed in Figure 2. Figure 2A shows that the surface of the untreated CNF has relatively smooth surface and a porous matrix with a relatively good dispersion is observable. Figure 2B illustrates that the surface morphology of the CNF changed after the modification with 0.5 wt% phthalimide, where the surface of the CNF presents an integrated structure and no surface change is observed that indicating phthalimide grafted on CNF. Figure 2C shows that the surface of the fiber changes significantly after increasing the fraction of phthalimide (1 wt%). Indeed, more uniform surface developed and the number of interruptions and gap size decreased accompanied by the development of sheet-

TABLE 1 Density and crystallinity index of CNF and CNF-Ph aerogels

Sample	Density (g/cm^3)	CrI (%)
CNF	0.0105[a],*	76.0
CNF-Ph0.5	0.0112[a]	74.0
CNF-Ph1.0	0.0138[b]	68.7
CNF-Ph1.5	0.0164[c]	65.2

*Different lowercase letters in the same column show the significant difference ($P < .05$).

like configuration. Figure 2D shows at a higher phthalimide loading (1.5 wt%), more phthalimide entrapped within the CNF fibrils and more sheet-like structure could be observed, which causes an increase of the surface area.

3.2 | Aerogel density

The results of ANOVAs showed significant effect of different phthalimide loadings on density of the resulting aerogels at 95% confidence level. Furthermore, based on Duncan multiple range test results provided in Table 1, at lower phthalimide loadings (0.5%), the difference in mean density is not significant, but at higher loadings (more than 0.5%), there is significant difference in the mentioned attributes. In

other words, the results showed that with surface modification and increasing phthalimide loading, density increased.

3.3 | X-ray diffraction

Figure 3 shows the diffractograms of CNF and CNF-Ph aerogels. All the diffractograms displayed the typical peaks of semicrystalline material which consist of broad hump of the amorphous region and sharp intense peaks of the crystalline region.[19,20] Cellulose diffractogram showed three peaks around $2\theta = 16°$, $22.5°$, and $34.5°$ which are related to the cellulose I, corresponding to the (101), (002), and (040) crystallographic.[21,22] On the other hand, in the CNF diffractograms, the peaks at $2\theta = 22.5°$ are getting sharper and more intense, meaning that samples are more crystalline. The peak is used to relate to the crystallinity of the materials that can be used to calculate the CrI as shown by Equation (1).[23]

Table 1 shows the CrI of all samples. The CrI of CNF is 76%. The replacement of the hydroxyl groups by the amino groups of phthalimide resulted in the decrease of the compact crystalline regions of CNF during the chemical modification. Furthermore, the reduction of crystallinity as a result of CNF modification was stemmed from the replacement of the hydroxyl groups by groups of phthalimide that have larger size groups, which broke the inter- and intramolecular hydrogen bonds of CNF. As expected, with the increasing number of hydroxyl groups being replaced, the crystallinity decreased to somehow.

3.4 | Transmission electron microscopy

The TEM images of CNF before and after chemical modification are shown in Figure 4. As seen, the nanofibers have maintained their morphology after the phthalimide modification. Indeed, after modification of CNF, there is no distinguishable change in the structure of the fibers, but the density and the surface area of fibers increased with a relatively more uniform dispersion.

3.5 | Zeta potential

The zeta potential of both CNF and CNF-Ph was measured, and it appears that the pure CNF is negatively charged whereas the zeta potential of CNF-Ph is positive. This confirms the successful modification as CNF is essentially negatively charged due to hydroxyl groups ($-OH^-$) but after modification, it turns to positive charges as a result of the presence of amino groups ($-NH^+$). The absolute value of the zeta potential of the CNF-Ph solution is higher than that pure CNF solution (62.2 and -52.5 V, respectively), showing that the modified CNF solution is more stable than the unmodified CNF solution, maybe due to higher amount of hydroxyl groups in the latter.[24,25]

3.6 | Attenuated total reflectance-Fourier transform infrared

Phthalimide has a hydrophilic head ($-NH$) and a hydrophobic end; hence, CNF could create hydrogen bonds with the fiber surface at the hydrophilic head.[15] The possible mechanism is shown in Figure 5. The interaction between phthalimide and the CNF surfaces as studied by ATR-FTIR spectrometry and spectra is shown in Figure 6. The curve (A) represents the
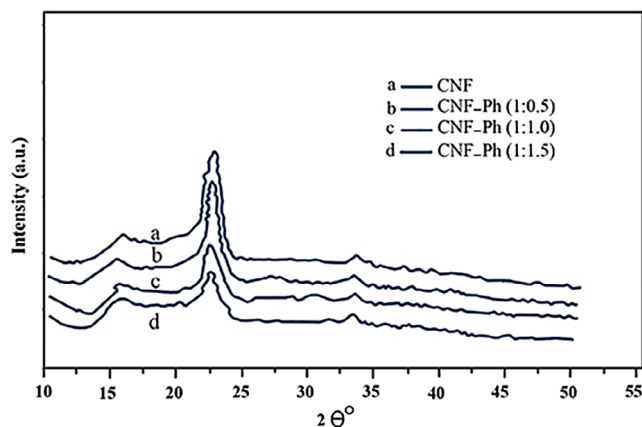
FIGURE 3 XRD analysis for CNF and CNF-Ph samples [Color figure can be viewed at wileyonlinelibrary.com]
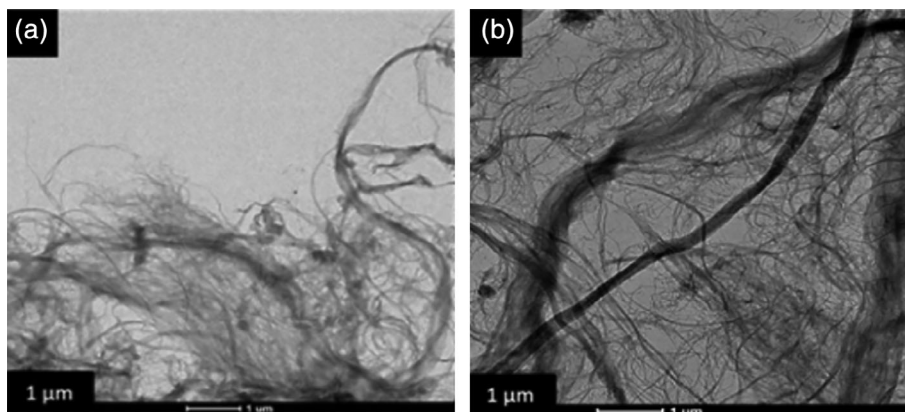
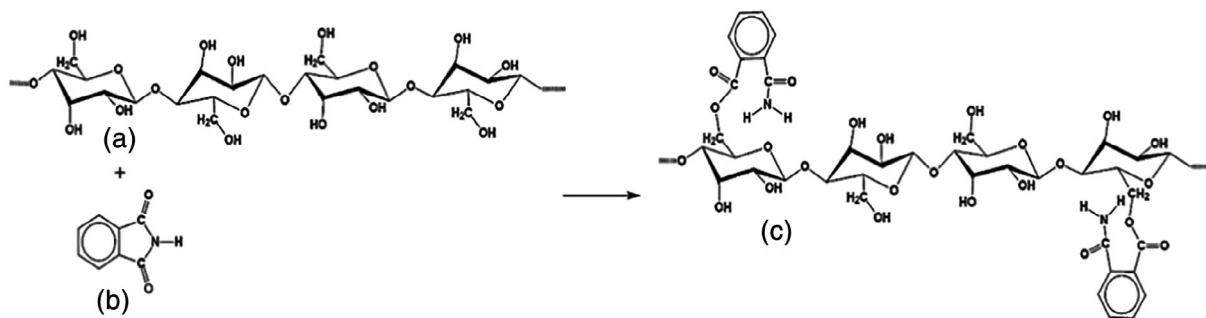**FIGURE 4** TEM images of (a) CNF and (b) CNF-Ph

FIGURE 5 Chemical reaction between CNF surface and phthalimide. a, CNF. b, Phthalimide. c, CNF-Ph[15]
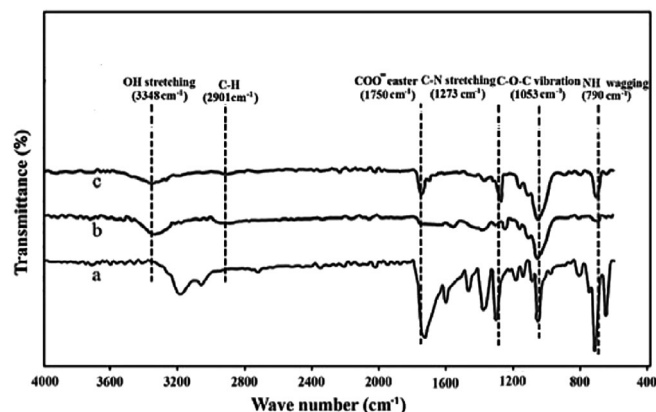

FIGURE 6 ATR-FTIR spectra of (A) Ph, (B) CNF, and (C) CNF-Ph

FIGURE 7 TGA result for CNF and CNF-Ph samples [Color figure can be viewed at wileyonlinelibrary.com]

spectrum for pure phthalimide. The 1600 cm^{-1} peak shows the stretching vibration of C=C bonds in the aromatic ring, and the 3305 and 1713 cm^{-1} peaks are related to the stretching vibrations of secondary N—H amide bands and conjugated C=O bonds, respectively.[15] The CNF spectrum (curve B) shows a number of characteristic bands such as O—H stretching at 3346 cm^{-1}, C—H stretching at 2901 cm^{-1}, and C—O—C skeletal vibrations at 1053 cm^{-1}, while O—H and C—H bending along with C—C and C—O stretching are located at 1376, 1310, and 1253 cm^{-1}, respectively. All the peaks are the typical peaks of cellulose.[26] The CNF-Ph (curves C) shows the emerging of small new peaks located at approximately 1750 cm^{-1} (1740-1750 cm^{-1}), 1273 cm^{-1} (1270-1273 cm^{-1}), and 790 cm^{-1} (780-790 cm^{-1}), which are attributed to ester bonding COO$^-$, C—N stretching, and NH$_2$ wagging, respectively. Thus, the existence of all the new peaks of the CNF spectrum indicates that chemical modification had happened and the phthalimide was grafted to the O—H functional groups on CNF surfaces.

3.7 | Thermogravimetric analysis

Thermal stability is often used to describe the thermal durability of a material. Figure 7 shows the TGA curves for CNF and CNF-Ph ae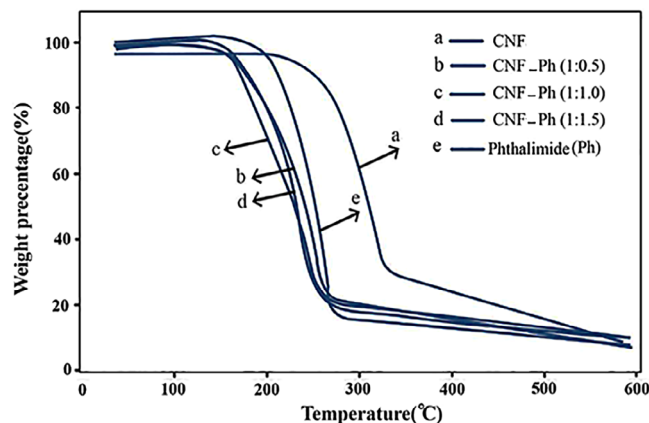rogels with various phthalimide loading ratios. The thermal decomposition of the CNF-Ph occurs at two weight loss stages. The first weight loss at low temperature, in a range lower than 100°C, is due to the vaporization of adsorbed and intermolecular H-bonded water.[26,27] The second stage between 250°C and 330°C corresponds to the pyrolysis of the CNF aerogel, this is dehydration and decomposition. The lower degradation temperature of CNF aerogel might be due to the heterogeneous distribution of fiber size where smaller fibers decompose at the lower temperature range (275°C-370°C).[28] The primary weight loss of CNF-Ph aerogels started approximately at 150°C. Indeed, increasing the phthalimide content resulted in a decrease of the decomposition temperature since phthalimide decomposition occurs at lower temperature of 250°C. In addition, it increases the weight loss (which was lower than the CNF at 250°C) due to its very active amino group which usually reduces the stability of polymer.[29] OH group on the CNF surface has reacted with amino groups (NH$_2$) of phthalimide. Since more energy is needed for breaking hydroxyl bonds than ionic bonds, by taking into account the reduced hydrogen bonds as the result of the chemical modification, the thermal stability of the CNF-Ph is lower than the CNF aerogels. TGA analysis revealed that when increasing amount of phthalimide groups, the thermal stability decreases. This
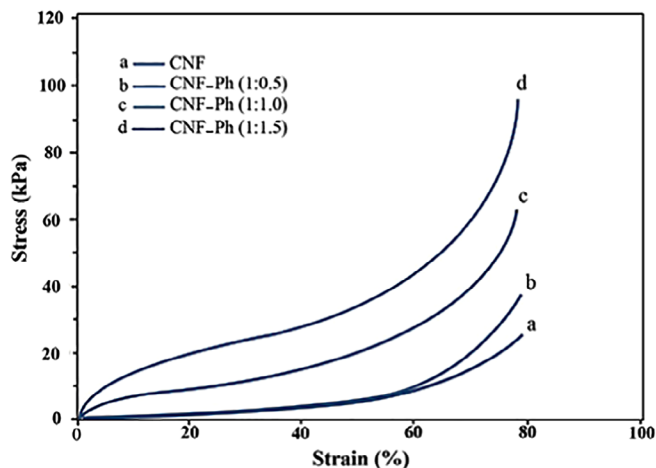
FIGURE 8   Compressive stress-strain curves of CNF and Ph-CNF samples [Color figure can be viewed at wileyonlinelibrary.com]

TABLE 2   Maximum stress and Young's modulus CNF and CNF-Ph aerogels

Sample	Density (g/cm^3)	Strength (kPa)	Young's modulus (kPa)	References
CNF	0.0105[a,*]	21.2[a]	26.7[a]	Present study
CNF-Ph0.5	0.0112[a]	35.7[b]	45.4	
CNF-Ph1.0	0.0138[b]	58.6[c]	72.3[c]	
CNF-Ph1.5	0.0164[c]	95.3[d]	110.8[d]	
CNF aerogel	0.0081	25.3	54.4	[32]
CNF aerogel	0.0106	30.49	36.13	[24]
	0.0137	54.75	64.88	
	0.1753	72.09	85.44	

*Different lowercase letters in the same column show the significant difference ($P < .05$).

could be attributed to the interaction between the CNF and phthalimide upon the modification of CNF.

3.8 | Mechanical properties

The mechanical properties of CNF and CNF-Ph aerogels with various densities (0.0105, 0.0112, 0.0138, and 0.0164 g/cm^{-3}) were studied. The compressive stress-strain of the prepared aerogels is presented in Figure 8. The stress-strain behavior was linear at low strain, and with increasing density, the slopes increase as well. The main deformation appears to be essentially stemmed from elastic cell wall bending, or even collapsing of major cellular pores. In other words, the resistance to compression is due to hydrogen bonds and physical crosslinks.[30] Under high strain, the aerogel deforms mainly because of the mesopores failure whereby the covalent bonds are compressed or broken. In these circumstances, due to the densification of the porous structure, the walls of the minor pores start to touch each other and become the loading-bearing portion.[24,30,31] The mechanical results are summarized in Table 2. For comparison, some data of other aerogels collected from the literature are included. Also, the modulus of elasticity increased as a result of increasing aerogel densities that it could be attributed to better elastic characteristics of materials with smaller pores and hence, more closely spaced pore walls. The relatively low values of maximum compressive stress and Young's modulus of the aerogels could be attributed to their very low densities and high porosities.[24]

4 | CONCLUSIONS

In this work, CNF was successfully modified with phthalimide in 96/4 (v/v) water/acetic acid solvent. Simple freeze-drying method was used to remove water directly from aqueous gel. The SEM results showed that surface morphology of the CNF was changed after the modification, and this confirms a proper interaction and conformity between CNF and phthalimide. Also, the ATR-FTIR analysis revealed three new peaks for COO^-, C—N, and NH_2 which is supporting grafting of phthalimide on CNF. The XRD results indicated that after introducing the phthalimide on the CNF surface, due to the replacement of hydroxyl groups by phthalimide, the crystallinity was relatively reduced. In addition, the thermal stability of the modified CNF was decreased; this is due to replacement of OH groups in CNF by NH_2 groups in phthalimide. Surface morphology of the CNF changed after the modification with 0.5 wt% phthalimide, where the surface of the CNF presents an integrated structure and no surface change is observed that indicating phthalimide grafted on CNF.

ORCID

Alireza Ashori https://orcid.org/0000-0003-0946-1965

REFERENCES

[1] S. Eyley, W. Thielemans, *Nanoscale* **2014**, *6*, 7764.

[2] N. Lin, A. Dufresne, *Biomacromolecules* **2013**, *14*, 871.

[3] A. Hajlane, Luleå University of Technology Department of Engineering Sciences and Mathematics Division of Materials Science. (**2014**) 1.

[4] A. Tayeb, E. Amini, S. Ghasemi, M. Tajvidi, *Molecules* **2018**, *23*, 2684.

[5] S. Kuga, *Chromatography A* **1980**, *195*, 221.

[6] U. J. Kim, S. Kuga, *Cellulose* **2000**, *7*, 287.

[7] G. S. Chauhan, H. Lal, *Desalination* **2003**, *159*, 131.

[8] C. Salas, T. Nypelo, C. RodriguezAbreu, C. Carrillo, O. J. Rojas, *Curr. Opin. Colloid Interface Sci.* **2014**, *19*, 383.

[9] P.A. Gale, and C.J.E. Haynes, *Wiley-Blackwell 287*, London (**2012**).

[10] S. Hokkanen, E. Repo, M. Sillanpää, *J. Chem. Eng.* **2013**, *223*, 40.

[11] S. Kalia, S. Boufi, A. Celli, S. Kango, *Colloid Polym. Sci.* **2014**, *292*, 5.

[12] H. Khanjanzadeh, R. Behrooz, N. Bahramifar, W. Gindl-Altmutter, M. Bacher, M. Edler, T. Griesser, *Biomacromolecules* **2018**, *106*, 1288.

[13] H. Khanjanzadeh, R. Behrooz, N. Bahramifar, S. Pinkl, W. Gindl-Altmutter, *Carbohydr. Polym.* **2019**, *206*, 11.

[14] J. Lu, P. Askeland, L. T. Drzal, *Polymer* **2008**, *49*, 1285.

[15] P. Marzbani, H. Resalati, A. Ghasemian, A. Shakeri, *Bioresources* **2016**, *11*, 8720.

[16] N. H. Mohad, N. F. Hadina Ismail, J. I. Zahari, W. F. Wan Fathilah, H. Karagarzadeh, S. Ramli, I. Ahmad, A. M. Yarmo, R. Othman, *J. Nanomater.* **2016**, *2016*, 8720.

[17] N. Mahfoudhi, S. A. Boufi, *Cellulose* **2017**, *24*, 1171.

[18] L. Segal, J. Creely, A. Martin, C. Conrad, *Text. Res. J.* **1959**, *29*, 786.

[19] H. Kargarzadeh, I. Ahmad, I. Abdullah, A. Dufresne, S. Y. Zainudin, R. M. Sheltami, *Cellulose* **2012**, *19*, 855.

[20] A. Samzadeh Kermani, N. Esfandiary, *J. Adv. Nanopart.* **2016**, *5*, 18.

[21] N. N. Ngadi, S. Lani, *J. Sci. Eng.* **2014**, *68*, 35.

[22] C. Tian, S. Fu, J. Chen, Q. Meng, L. A. Lucia, *Nordic Pulp Pap. Res. J.* **2014**, *29*, 58.

[23] M. S. Nazir, B. A. Wahjoedi, A. W. Yussof, M. A. Abdullah, *Bioresources* **2013**, *8*, 2161.

[24] F. Rafieian, M. Hosseini, M. Jonoobi, Q. Yu, *Cellulose* **2018**, *25*, 4695.

[25] M. Rinaudo, *J. Appl. Polym. Sci.* **1993**, *52*, 11.

[26] A. Kumar, Y. S. Negi, V. Choudhary, N. K. Bhardwaj, *J. Mater. Phys. Chem.* **2014**, *2*, 1.

[27] A. Arbelaiz, B. Fernandez, J. Ramos, I. Mondragon, *J. Therm. Acta* **2006**, *440*, 111.

[28] M. R. K. Sofla, R. J. Brown, T. Tsuzki, T. J. Rainey, *J. Adv. Nat. Sci Nanosci. Nanotechnol.* **2016**, *7*, 1.

[29] N. Li, H. Wang, X. Qu, Y. Chen, *J. Mar. Drugs* **2017**, *15*, 1.

[30] Y. Si, J. Yu, X. Tang, J. Ge, B. Ding, *J. Nat. Commun.* **2014**, *5*, 1.

[31] X. Yang, E. D. Cranston, *J. Chem. Mater.* **2014**, *26*, 6016.

[32] F. Jiang, Y. L. Hsieh, *J. Mater. Chem. A* **2014**, *2*, 6337.